MultiCraft

International Journal of Engineering, Science and Technology
Vol. 5, No. 4, 2013, pp. 80-99

INTERNATIONAL JOURNAL OF ENGINEERING, SCIENCE AND TECHNOLOGY

www.ijest-ng.com
www.ajol.info/index.php/ijest

Optimum material gradient composition for the functionally graded piezoelectric beams

M. Lezgy-Nazargah[1], M. Farahbakhsh[2]

[1, 2]Department of Civil Engineering, Hakim Sabzevari University, Tovhidshahr, Sabzevar, IRAN*
[*]Corresponding Author: e-mails: m.lezgy@hsu.ac.ir & m.lezgy.n@gmail.com, Fax: 0098(571)4003520, Tel: 0098(571)4003527
(e-mail:mostafa.farahbakhsh.69@gmail.com)

Abstract

This study investigates the relation between the material gradient properties and the optimum sensing/actuation design of the functionally graded piezoelectric beams. Three-dimensional (3D) finite element analysis has been employed for the prediction of an optimum composition profile in these types of sensors and actuators. To this end, various static tests for functionally graded piezoelectric beams with different geometric parameters, material gradient index, mechanical and electrical boundary conditions are considered. The obtained numerical results of the present study not only would help the selection of a most suitable volume fraction distribution for the functionally graded piezoelectric sensors and actuators but also give a comprehensive insight about the static electro-mechanical behavior of these structures. Moreover, the present results could serve as a benchmark to assess different one-dimensional functionally graded piezoelectric beam theories.

Keywords: Piezoelectric sensors and actuators, Functionally graded materials, Stress minimization, Optimum design, Finite element method

DOI: http://dx.doi.org/10.4314/ijest.v5i4.8

1. Introduction

In recent years, piezoelectric materials have been found much application in intelligent structures in view of their capabilities of sensing and actuating. Accurate simulation and theoretical modeling of intelligent structures has been an intensive area of research for more than two decades. Extensive studies have been carried out, and many theoretical and mathematical models have been presented for laminated composite structures with piezoelectric sensors and actuators until now (Tzou and Tseng, 1990; Pablo et al., 2009; D'Ottavio and Polit, 2009; Vidal et al., 2011; Beheshti-Aval and Lezgy-Nazargah, 2010a,b; Beheshti-Aval et al., 2011; Beheshti-Aval and Lezgy-Nazargah, 2012a,b; Niezrecki et al., 2001).

In order to achieve large deformations, the piezoelectric actuators are often made of several layers of different piezoelectric materials. Although this conventional type of design may provide larger deformations, it has several restricting disadvantages that reduce its reliability. For the piezoelectric actuators made of different piezoelectric layers or identical piezoelectric layers with different poling directions, high stress concentrations are usually appeared at the layer interfaces under mechanical or electrical loading. These stress concentrations lead to the initiation and propagation of micro-cracks near the interfaces of two bonded piezoelectric layers. Such drawbacks reduce lifetime and the reliability of these structures. To reduce the limitations of the conventional piezoelectric laminates, sensors and actuators with graded properties was introduced and fabricated by Zhu and Meng (1995), and Wu et al. (1996). A functionally graded piezoelectric is a kind of piezoelectric materials whose mechanical and electrical properties vary continuously in one or more directions. Functionally graded piezoelectric actuators can produce not only large displacements but also reduce the internal stress concentrations and consequently improve significantly the lifetime of piezoelectric actuators. Now, the functionally graded piezoelectric materials, as intelligent materials, have been used extensively in applications of sensors and actuators in the micro-electro-mechanical system and smart structures.

There exist already a considerable number of papers treating the static and dynamic behavior of functionally graded piezoelectric sensors and actuators. Lim and He (2001) obtained an exact solution for a compositionally graded piezoelectric layer under uniform stretch, bending and twisting load. Reddy and Cheng (2001) obtained a 3D solution for smart functionally gradient plates. Zhong and Shang (2003) presented an exact 3D solution for functionally graded piezoelectric rectangular plates, by means of the state space approach. Lu et al. (2005) presented an exact solution for simply supported functionally graded piezoelectric laminates in cylindrical bending by Stroh-like formalism. Using this method, Lu et al. (2006) also proposed the exact solutions for simply supported functionally graded piezoelectric plates. Liu and Shi (2004), and Shi and Chen (2004) obtained closed form solutions for the functionally graded piezoelectric cantilever beams using the two-dimensional (2D) theory of elasticity and the Airy stress function. Xiang and Shi (2009) investigated the thermo-electro-elastic response of a functionally graded piezoelectric sandwich cantilever beam. They employed also the Airy stress function in order to study the effect of parameters such as the electromechanical coupling, functionally graded index, temperature change and thickness ratio on the static behavior of actuators/sensors. Using the so called state-space based differential quadrature method (SSDQM), Li and Shi (2009) investigated the free vibration of a functionally graded piezoelectric beam. Lee (2005) used a layerwise finite element formulation in order to investigate the displacement and stress response of a functionally graded piezoelectric bimorph actuator. By using the Timoshenko beam theory, Yang and Xiang (2007) investigated the static and dynamic response of functionally graded piezoelectric actuators under thermo-electro-mechanical loadings.

A comprehensive study on the static, dynamic and free vibration response of functionally graded piezoelectric panels under different sets of mechanical, thermal and electrical loadings using the finite element method was presented by Behjat et al. (2009). Behjat et al. (2011) investigated also the static bending; free vibration and dynamic response of functionally graded piezoelectric plates under mechanical and electrical loads using the first order shear deformation theory. Wu et al. (2002) derived a high-order theory for functionally graded piezoelectric shells based on the generalized Hamilton's principle. Lezgy-Nazargah et al. (2013) proposed an efficient finite element model for static and dynamic analyses of functionally graded piezoelectric beams. They used an efficient three-nodded beam element which is based on a refined sinus model. The proposed beam element of these researchers does not require shear correction factor and ensures continuity conditions for displacements, transverse shear stresses as well as boundary conditions on the upper and lower surfaces of the functionally graded piezoelectric beam. Bodaghi and Shakeri (2012) analytically investigated the free vibration and dynamic response of simply supported functionally graded piezoelectric cylindrical panel impacted by time-dependent blast pulses. Using Hamilton's principle, they derived the equations of motion based on the first-order shear deformation theory. In the work of these researchers, Maxwell's electricity equation is taken as one of the governing equations. Bodaghi et al. (2012) investigated the non-linear active control of the dynamic response of functionally graded beams with rectangular cross-section in thermal environments exposed to blast loadings. They derived non-linear equations of motion of the smart beam based on the first-order shear deformation theory and the von Karman geometrical non-linearity.

In the development of modern structures, optimization is an essential topic for many engineering field. Although functionally graded piezoelectric materials have been proposed as a potential upgrade to some conventional piezoelectric sensors/actuators, to design the functionally graded piezoelectric sensors/actuators with enhanced properties and mechanical reliability, it is necessary to determine their optimum composition profile. The behavior of functionally graded piezoelectric materials under electro-mechanical loadings is significantly affected by the choice of volume fraction distributions within the graded layer. Therefore, the selection of a suitable volume fraction distribution is an essential part for designing functionally graded piezoelectric sensors and actuators. However, the rare studies can be found in this subject in the literature. Therefore, volume fraction optimization of functionally graded piezoelectric sensors and actuators is to investigate in this study. In the present paper, 3D finite element method is selected for simulating of electro-mechanical behaviors of functionally graded piezoelectric sensors and actuators. For the various length to thickness ratios, volume fraction distributions, electrical and mechanical boundary conditions, static electro-mechanical bending analysis are performed. Finally, the relation between different functionally gradient material properties and the best performance of the functionally graded piezoelectric actuator\sensor, i.e. large bending\sensing while reducing the induced stress fields is investigated. The obtained numerical results of the present study give a comprehensive insight about the static behavior of the functionally graded piezoelectric sensors and actuators. These obtained numerical results can be also used to assess the accuracy of different functionally graded piezoelectric beams theories and/or validating finite element codes.

2. Geometry and coordinate system

The considered beam is a prismatic one with a rectangular uniform cross section of width *b*, height *h*, length *L* and made of functionally graded piezoelectric materials. The geometric parameters of the functionally graded piezoelectric beam and the chosen Cartesian coordinate system (x_1, x_2, x_3) are shown in Figure 1.

3. Constitutive equations

The 3D linear constitutive equations of the functionally graded piezoelectric beam, polarized along its thickness direction in its global material coordinate system can be expressed as:

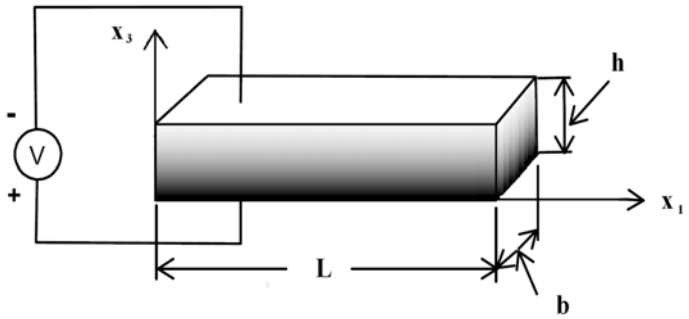

Figure 1. Functionally graded piezoelectric beam: Cartesian coordinate system and geometric parameters

$$\begin{Bmatrix}\sigma_{11}\\ \sigma_{22}\\ \sigma_{33}\\ \sigma_{23}\\ \sigma_{13}\\ \sigma_{12}\end{Bmatrix}=\begin{bmatrix}c_{11} & c_{12} & c_{13} & 0 & 0 & c_{16}\\ c_{12} & c_{22} & c_{23} & 0 & 0 & c_{26}\\ c_{13} & c_{23} & c_{33} & 0 & 0 & c_{36}\\ 0 & 0 & 0 & c_{44} & c_{45} & 0\\ 0 & 0 & 0 & c_{45} & c_{55} & 0\\ c_{16} & c_{26} & c_{36} & 0 & 0 & c_{66}\end{bmatrix}\begin{Bmatrix}\varepsilon_{11}\\ \varepsilon_{22}\\ \varepsilon_{33}\\ 2\varepsilon_{23}\\ 2\varepsilon_{13}\\ 2\varepsilon_{12}\end{Bmatrix}-\begin{bmatrix}0 & 0 & e_{31}\\ 0 & 0 & e_{32}\\ 0 & 0 & e_{33}\\ e_{14} & e_{24} & 0\\ e_{15} & e_{25} & 0\\ 0 & 0 & e_{36}\end{bmatrix}\begin{Bmatrix}E_1\\ E_2\\ E_3\end{Bmatrix} \tag{1}$$

$$\begin{Bmatrix}D_1\\ D_2\\ D_3\end{Bmatrix}=\begin{bmatrix}0 & 0 & 0 & e_{14} & e_{15} & 0\\ 0 & 0 & 0 & e_{24} & e_{25} & 0\\ e_{31} & e_{32} & e_{33} & 0 & 0 & e_{36}\end{bmatrix}\begin{Bmatrix}\varepsilon_{11}\\ \varepsilon_{22}\\ \varepsilon_{33}\\ 2\varepsilon_{23}\\ 2\varepsilon_{13}\\ 2\varepsilon_{12}\end{Bmatrix}+\begin{bmatrix}\chi_{11} & \chi_{12} & 0\\ \chi_{12} & \chi_{22} & 0\\ 0 & 0 & \chi_{33}\end{bmatrix}\begin{Bmatrix}E_1\\ E_2\\ E_3\end{Bmatrix} \tag{2}$$

where σ_{ij}, ε_{ij} and E_i denote the stress tensor, the infinitesimal strain tensor and the electric field components respectively. D_i are the electric displacement vector components, and c_{kl}, e_{ik}, χ_{ij} elastic, piezoelectric and dielectric material constants. Unlike the homogeneous piezoelectric materials, c_{kl}, e_{ik} and χ_{ij} are now functions of the coordinate x_3. In the present study, we consider the material properties having the following exponential distributions:

$$c_{kl}=c_{kl}^0 e^{a_1(x_3/h)},\quad e_{ik}=e_{ik}^0 e^{a_2(x_3/h)},\quad \chi_{ij}=\chi_{ij}^0 e^{a_3(x_3/h)} \qquad i,j=1,2,3 \qquad k,l=1,2,.....,6 \tag{3}$$

where c_{kl}^0, e_{ik}^0 and χ_{ij}^0 are the values of material properties at the plane $x_3=0$, a_1, a_2 and a_3 are the material property gradient indexes which can be determined by the values of the material properties at the planes, $x_3=0$ and $x_3=h$, i.e.

$$a_1=\ln c_{kl}^h-\ln c_{kl}^0,\ a_2=\ln e_{ik}^h-\ln e_{ik}^0,\ a_3=\ln \chi_{ij}^h-\ln \chi_{ij}^0 \tag{4}$$

The assumption that the material properties vary exponentially with spatial position is not only simple for treatment, it also provides some essential features of functionally gradient materials. Therefore, it was employed by many researchers to model the elastic or thermoelastic behaviors of functionally graded material (e.g., Erdogan, (1985); Delale and Erdogan (1888); Noda and Jin (1993); Gu and Asaro (1997); among others). Although it is not clear that an exponential distribution is the one that will allow an optimization of the material response, this distribution has been employed in most of practical and theoretical studies. In the other words, it may be possible that a special distribution other than exponential distribution leads to an optimization of the material response, but the manufacture of a functionally graded piezoelectric sensor/actuator with a special distribution will be very expensive or applicability impossible. To this reason, in the present study we are seeking the optimum material gradient composition for the most popular type of functionally graded piezoelectric sensors/actuators which are functionally graded piezoelectric materials with the exponential distribution.

The constitutive relations (1) and (2) could be expressed as the following compact form:

$$\boldsymbol{\sigma}=\boldsymbol{C}\,\boldsymbol{\varepsilon}-\boldsymbol{e}^{\boldsymbol{T}}\,\boldsymbol{E}$$
$$\boldsymbol{D}=\boldsymbol{e}\,\boldsymbol{\varepsilon}+\boldsymbol{\chi}\,\boldsymbol{E} \tag{5}$$

where

$$\boldsymbol{\sigma}=\{\sigma_{11}\quad \sigma_{22}\quad \sigma_{33}\quad \sigma_{23}\quad \sigma_{13}\quad \sigma_{12}\}^T,\quad \boldsymbol{D}=\{D_1\quad D_2\quad D_3\}$$

$$\boldsymbol{\varepsilon} = \{\varepsilon_{11} \quad \varepsilon_{22} \quad \varepsilon_{33} \quad 2\varepsilon_{23} \quad 2\varepsilon_{13} \quad 2\varepsilon_{12}\}^T , \qquad \boldsymbol{E} = \{E_1 \quad E_2 \quad E_3\}$$

$$\boldsymbol{C} = \begin{bmatrix} c_{11} & c_{12} & c_{13} & 0 & 0 & c_{16} \\ c_{12} & c_{22} & c_{23} & 0 & 0 & c_{26} \\ c_{13} & c_{23} & c_{33} & 0 & 0 & c_{36} \\ 0 & 0 & 0 & c_{44} & c_{45} & 0 \\ 0 & 0 & 0 & c_{45} & c_{55} & 0 \\ c_{16} & c_{26} & c_{36} & 0 & 0 & c_{66} \end{bmatrix}$$

$$\boldsymbol{e} = \begin{bmatrix} 0 & 0 & 0 & e_{14} & e_{15} & 0 \\ 0 & 0 & 0 & e_{24} & e_{25} & 0 \\ e_{31} & e_{32} & e_{33} & 0 & 0 & e_{36} \end{bmatrix}$$

$$\boldsymbol{\chi} = \begin{bmatrix} \chi_{11} & \chi_{12} & 0 \\ \chi_{12} & \chi_{22} & 0 \\ 0 & 0 & \chi_{33} \end{bmatrix}$$

4. Finite element modeling

The finite element model used for studying the behavior of the functionally graded piezoelectric beam (Figure 1) is a 20-node piezoelectric solid element. For each node, there are four degrees of freedom: one for electric potential and three for translations along the global coordinate axes of x_1, x_2, and x_3. For a 20-node coupled finite element with four degrees of freedom per node, strain and electric field components may be expressed in the following matrices form:

$$\begin{bmatrix} \boldsymbol{\varepsilon} \\ \boldsymbol{E} \end{bmatrix} = \begin{bmatrix} \boldsymbol{L}_{uu} & \boldsymbol{0} \\ \boldsymbol{0} & \boldsymbol{L}_{\varphi\varphi} \end{bmatrix} \begin{bmatrix} \boldsymbol{u} \\ \boldsymbol{\varphi} \end{bmatrix} \tag{6}$$

where

$$\boldsymbol{u} = [u \quad v \quad w]^T , \qquad \boldsymbol{\varphi} = [\phi]^T$$

$$\boldsymbol{\varepsilon} = [\varepsilon_{11} \quad \varepsilon_{22} \quad \varepsilon_{33} \quad 2\varepsilon_{23} \quad 2\varepsilon_{13} \quad 2\varepsilon_{12}]^T , \qquad \boldsymbol{E} = [E_1 \quad E_2 \quad E_3]^T$$

$$\boldsymbol{L}_{uu} = \begin{bmatrix} \partial/\partial x & 0 & 0 \\ 0 & \partial/\partial y & 0 \\ 0 & 0 & \partial/\partial z \\ 0 & \partial/\partial z & \partial/\partial y \\ \partial/\partial z & 0 & \partial/\partial x \\ \partial/\partial y & \partial/\partial x & 0 \end{bmatrix} , \quad \boldsymbol{L}_{\varphi\varphi} = \begin{bmatrix} -\partial/\partial x \\ -\partial/\partial y \\ -\partial/\partial z \end{bmatrix}$$

Due to this fact that the displacement components of a functionally graded piezoelectric beam are very small, the linear strain-displacement relations are employed in Eq. (6). The vector of displacement and electric potential components $\boldsymbol{u}$ and $\boldsymbol{\varphi}$ may be expressed in terms of the mechanical and electrical nodal variables vectors $\boldsymbol{u}_u^e$ and $\boldsymbol{u}_\varphi^e$ as follows:

$$\begin{bmatrix} \boldsymbol{u} \\ \boldsymbol{\varphi} \end{bmatrix} = \begin{bmatrix} \boldsymbol{N}_{uu} & \boldsymbol{0} \\ \boldsymbol{0} & \boldsymbol{N}_{\varphi\varphi} \end{bmatrix} \begin{bmatrix} \boldsymbol{u}_u^e \\ \boldsymbol{u}_\varphi^e \end{bmatrix} \tag{7}$$

where

$$\boldsymbol{u}_u^e = \{u_1 \quad u_2 \quad \cdots \quad u_{20} \quad \vdots \quad v_1 \quad v_2 \quad \cdots \quad v_{20} \quad \vdots \quad w_1 \quad w_2 \quad \cdots \quad w_{20}\}^T$$

$$\boldsymbol{u}_\phi^e = \{\phi_1 \quad \phi_2 \quad \cdots \quad \phi_{20}\}^T$$

$\boldsymbol{N}_{uu}$ and $\boldsymbol{N}_{\varphi\varphi}$ denote displacements and electric potential interpolation matrices, respectively. For the sake of brevity, the expression for $\boldsymbol{N}_{uu}$ and $\boldsymbol{N}_{\varphi\varphi}$ are not presented here. For further details, the readers are refereed to (Bathe, 1982). Eq. (7) can be rewritten as:

$$\{\boldsymbol{u} \quad \boldsymbol{\varphi}\}^T = \mathcal{N}\boldsymbol{u}^e \tag{8}$$

where

$\boldsymbol{u}^e = \{\boldsymbol{u}_u^e \quad \boldsymbol{u}_\phi^e\}^T$

and $\mathscr{N}$ denotes displacements and electric potential interpolation matrix. Using Eqs. (7) and (8), strain and electric field vectors may be expressed as follows:

$$\begin{bmatrix}\boldsymbol{\varepsilon}\\ \boldsymbol{E}\end{bmatrix}=\begin{bmatrix}\boldsymbol{L}_{uu} & \boldsymbol{0}\\ \boldsymbol{0} & \boldsymbol{L}_{\varphi\varphi}\end{bmatrix}\begin{bmatrix}\boldsymbol{u}\\ \boldsymbol{\varphi}\end{bmatrix}=\begin{bmatrix}\boldsymbol{L}_{uu} & \boldsymbol{0}\\ \boldsymbol{0} & \boldsymbol{L}_{\varphi\varphi}\end{bmatrix}\begin{bmatrix}\boldsymbol{N}_{uu} & \boldsymbol{0}\\ \boldsymbol{0} & \boldsymbol{N}_{\varphi\varphi}\end{bmatrix}\begin{bmatrix}\boldsymbol{u}_u^e\\ \boldsymbol{u}_\varphi^e\end{bmatrix}=\mathscr{B}\,\boldsymbol{u}^e \tag{9}$$

where $\mathscr{B}$ denotes strains and electric fields interpolation matrix.

The principle of virtual work is employed to extract governing equations of the functionally graded piezoelectric finite element model. According to this principle, for a piezoelectric medium of volume Ω and regular boundary surface Γ, one may write (Benjeddou, 2000):

$$\begin{aligned}\delta\Pi = \delta U - \delta W = &-\int_\Omega \boldsymbol{\delta\varepsilon}^T\boldsymbol{\sigma}\,d\Omega+\int_\Gamma \boldsymbol{\delta u}^T\boldsymbol{F}_S\,d\Gamma+\int_\Omega \boldsymbol{\delta u}^T\boldsymbol{F}_V\,d\Omega\\ &+\int_\Omega \delta\boldsymbol{E}^T\boldsymbol{D}\,d\Omega-\int_\Gamma \overline{Q}\,\delta\boldsymbol{\varphi}\,d\Gamma-\int_\Omega \overline{q}\,\delta\boldsymbol{\varphi}\,d\Omega=0\end{aligned} \tag{10}$$

where $\boldsymbol{F}_S$, $\boldsymbol{F}_V$, $\overline{q}$, $\overline{Q}$ and ρ are surface force vector, mechanical body force vector, electrical body charge, surface charge and mass density, respectively. $\delta\boldsymbol{u}$ and $\delta\boldsymbol{\varphi}$ are admissible virtual displacement and potential. Substituting Eqs. (5), (8) and (9) into Eq. (10), and assembling the element equations yields the following general equation:

$$\boldsymbol{K}\,\boldsymbol{q}(t)=\boldsymbol{F}(t) \tag{11}$$

The matrices and vectors in the above equation are elastic stiffness matrix $\boldsymbol{K}=\int_\Omega \mathscr{B}^T\begin{bmatrix}\boldsymbol{C} & -\boldsymbol{e}^T\\ \boldsymbol{e} & \boldsymbol{\chi}\end{bmatrix}\mathscr{B}\,d\Omega$, and loads vector $\boldsymbol{F}(t)=\int_\Omega \mathscr{N}^T\begin{bmatrix}\boldsymbol{F}_V\\ -\overline{q}\end{bmatrix}d\Omega+\int_\Gamma \mathscr{N}^T\begin{bmatrix}\boldsymbol{F}_S\\ -\overline{Q}\end{bmatrix}d\Gamma$.

5. Model verification

Verification of the simulating method explained in the previous section is essential before any study on the functionally graded piezoelectric beams. For this reason, a simply supported functionally graded piezoelectric square plate (*h=0.1m, X=Y=1m*) is analyzed using the 3D finite element model and the results are compared with exact 3D piezoelasticity results (Zhong and Shang, 2003). The plate is made of a PZT-4 based exponentially graded piezoelectric with the material properties cited in Table 1. The material property gradient indexes (a_1, a_2 and a_3) of this functionally graded piezoelectric plate are assumed to be 1.

Table 1. Mechanical and electrical properties of PZT-4 (Zhong and Shang, 2003)

$c_{11}^0\,(GPa)$	139	$e_{15}^0\,(C\,m^{-2})$	12.7
$c_{12}^0\,(GPa)$	77.8	$e_{24}^0\,(C\,m^{-2})$	12.7
$c_{22}^0\,(GPa)$	139	$e_{31}^0\,(C\,m^{-2})$	-5.2
$c_{13}^0\,(GPa)$	74.3	$e_{32}^0\,(C\,m^{-2})$	-5.2
$c_{23}^0\,(GPa)$	74.3	$e_{33}^0\,(C\,m^{-2})$	15.1
$c_{33}^0\,(GPa)$	115	$\chi_{11}^0\,(10^{-8}F\,m^{-1})$	1.306
$c_{44}^0\,(GPa)$	25.6	$\chi_{22}^0\,(10^{-8}F\,m^{-1})$	1.306
$c_{55}^0\,(GPa)$	25.6	$\chi_{33}^0\,(10^{-8}F\,m^{-1})$	1.151
$c_{66}^0\,(GPa)$	30.6		

The functionally graded piezoelectric plate is first subjected to a sinusoidal load defined by $\sigma_{33}(x_1,x_2,h)=-(\sin\pi x_1/X)(\sin\pi x_2/Y)$. The electric boundary condition is assumed to be closed circuit (CC). Concerning the results, a coupled 3D finite element analysis was carried out using the 20-node piezoelectric solid element (C3D20RE) available in the ABAQUS software. To this end, the thickness of the functionally graded piezoelectric plate was discretized into several thin homogenous layers with different electrical and mechanical material properties. In order to achieve accurate results, a very refined mesh is considered. To this end, the functionally graded piezoelectric plate has been discretized into 5120 equal

elements. The results obtained using twice the above number of elements is found to be indistinguishable from these results. Through-the-thickness distributions of u_1 , u_3 , σ_{11} , σ_{13} , σ_{33} and φ at a chosen field point ($x_1 / X = 1/4,\ x_2 / Y = 1/4$) are shown in Figure 2. It is observed from Figure 2 that results obtained from the present model are in very good agreement with the exact solution.

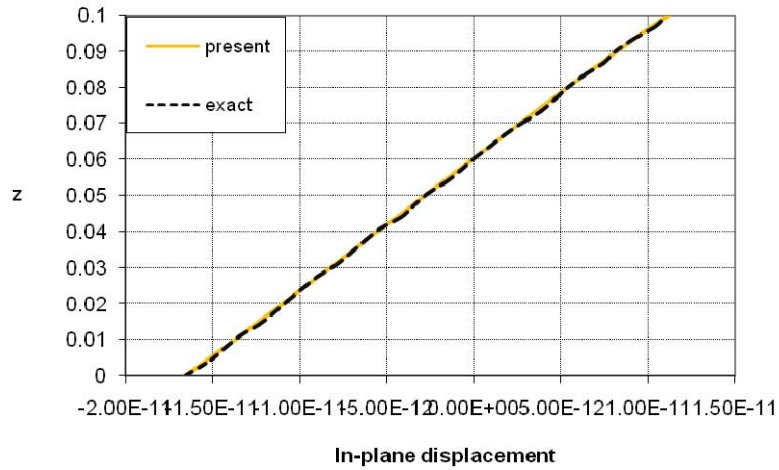

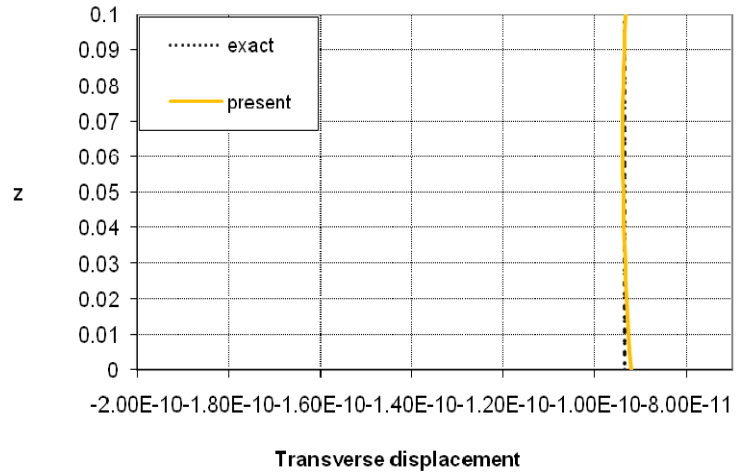

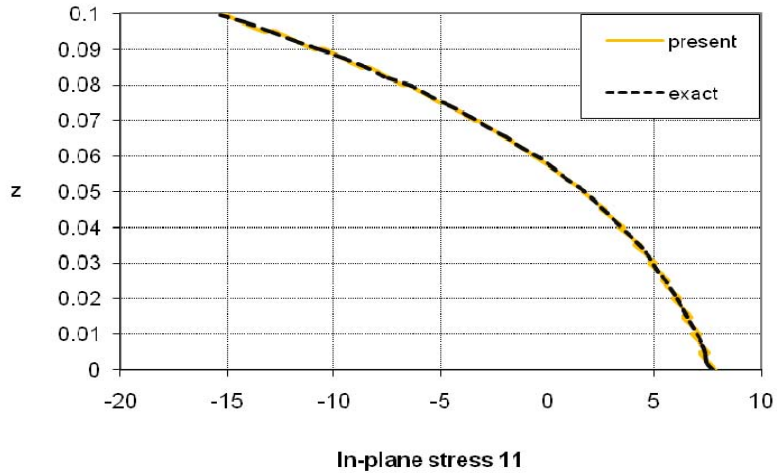

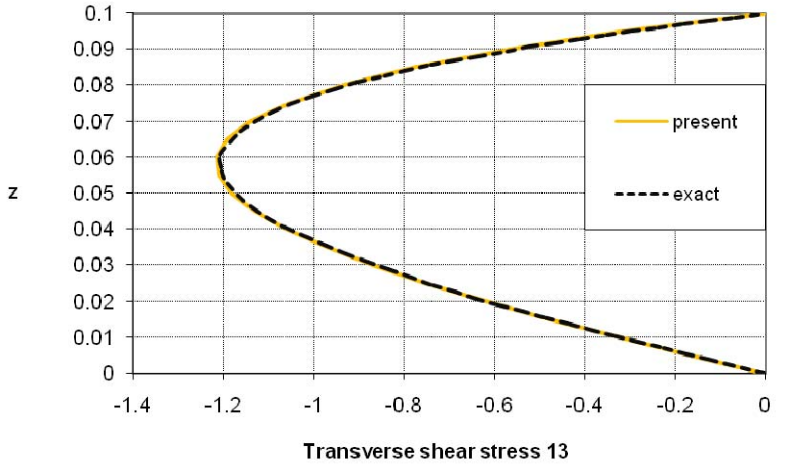

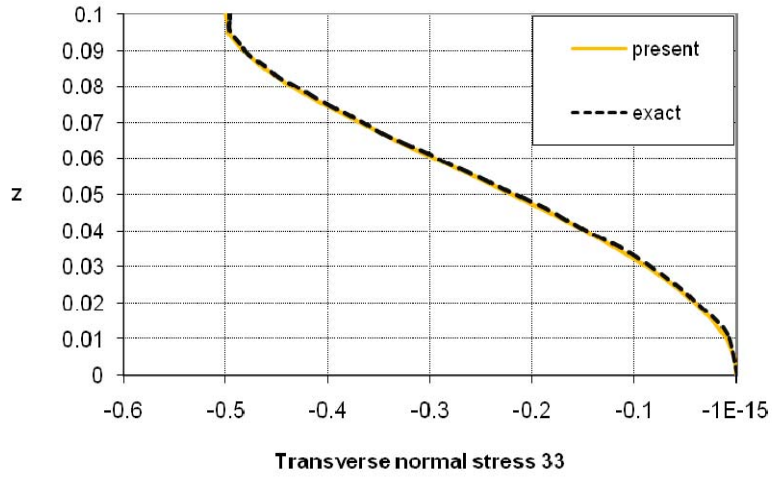

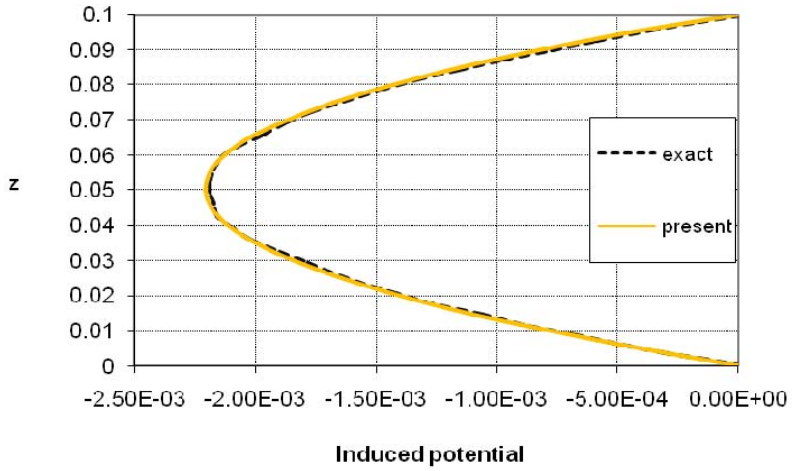

Figure 2. Through-the-thickness distributions of u_1 , u_3 , σ_{11} , σ_{13} , σ_{33} and φ in the simply supported functionally graded piezoelectric plate under the sinusoidal mechanical force at the chosen point $x_1/X = 1/4$, $x_2/Y = 1/4$.

In the next case, the electric potential $\varphi(x_1, x_2, h) = (\sin \pi x_1 / X)(\sin \pi x_2 / Y)$ is applied to the top of the functionally graded piezoelectric plate. The top and bottom surfaces of the beam are traction-free. The variation of σ_{11}, σ_{13} and D_3 are shown in Figure 3 as a function of the plate thickness coordinate x_3 at the chosen point $x_1 / X = 1/4$, $x_2 / Y = 1/4$. Similar to the sensor case, the exact piezoelasticity results have been also shown and compared with the present results in this figure. It is seen that the agreement between the present results with the exact solutions is excellent. These results demonstrate that the present 3D finite element is capable of simulating both the sensor and actuator behavior of functionally graded piezoelectric materials accurately.

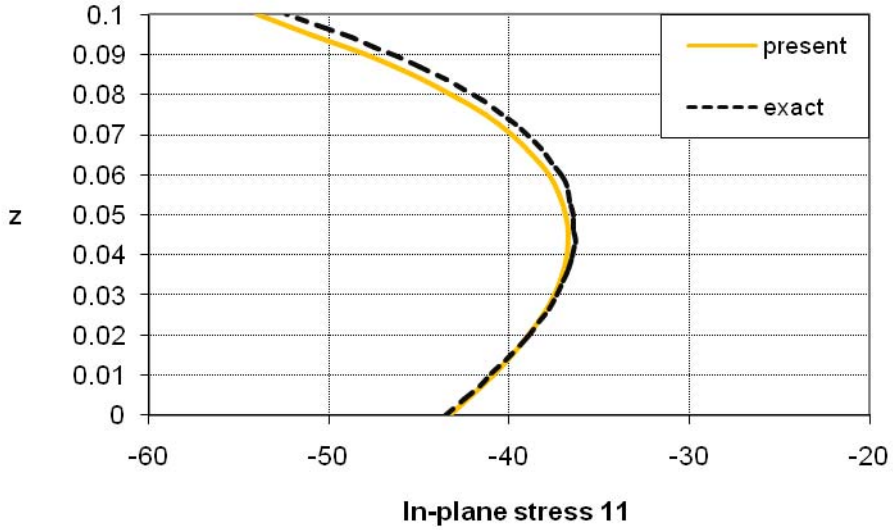

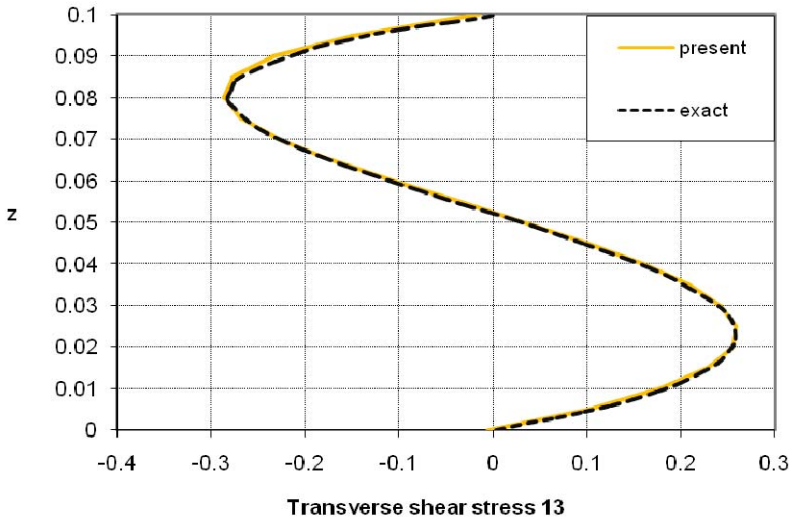

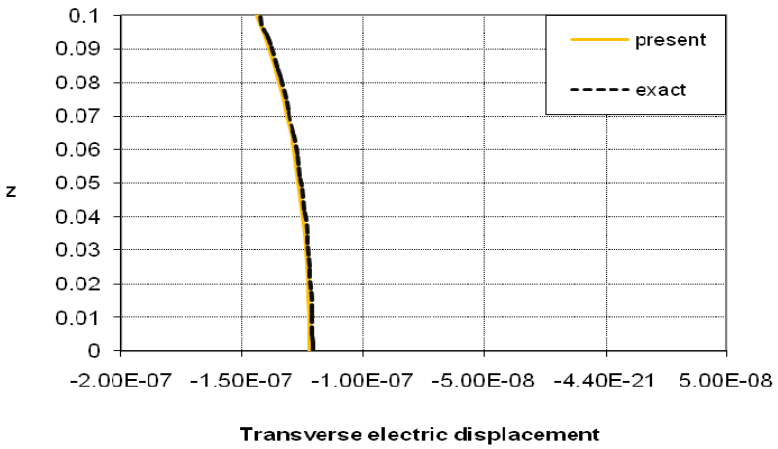

Figure 3. Through-the-thickness variations of σ_{11}, σ_{13} and D_3 in the functionally graded piezoelectric plate under the sinusoidal electric potential at the chosen point $x_1/X = 1/4$, $x_2/Y = 1/4$.

6. Results and discussions

Three groups of the functionally graded piezoelectric beams with three different mechanical boundary conditions clamped-free (C-F), simply support (S-S), and clamped-clamped (C-C) are considered. All of these beams have a wide of *b=1m* and a thickness of *h=1m* and is made of PZT-4 based exponentially graded piezoelectric. For the length to thickness ratio of these beams, five values of *L/h=1*, *L/h =5*, *L/h =10*, *L/h =20* and L/h=40 is considered. Considering these five length to thickness ratios seems to be enough for determining the optimum material gradient profile of functionally graded piezoelectric beams because thick, moderately thick and thin functionally graded piezoelectric beams are included in the analysis. Moreover, the electro-mechanical response of functionally graded piezoelectric beams with other length to thickness ratios may be predicted based on the numerical results available for the functionally graded piezoelectric beams with the above considered length to thickness ratios. For more simplicity, it is assumed that $a_1 = a_2 = a_3 = a$. These functionally graded piezoelectric beams have been analyzed using the 3D finite element model under electrical and mechanical loads. In order to achieve accurate results, a very refined mesh is considered. The mesh with 10000 elements is shown in Figure 4. The results obtained using twice the above numbers of elements are found to be indistinguishable from these results.

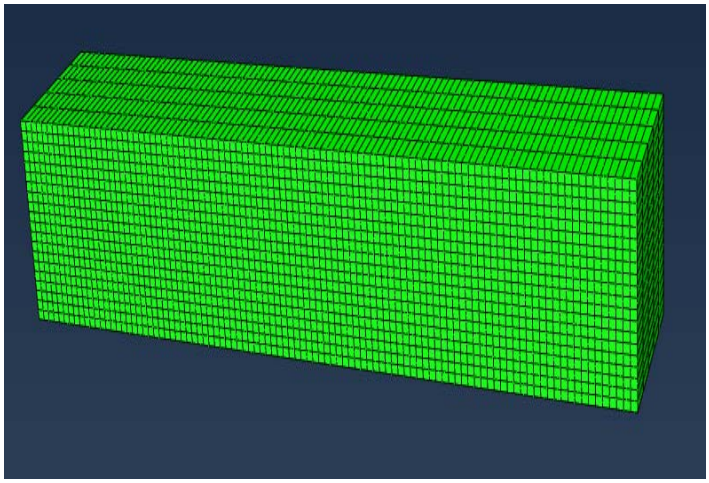

Figure 4. Functionally graded piezoelectric beam; mesh with 10000 elements (ABAQUS); L/h=5

The functionally graded piezoelectric beams are first subjected under the action of a uniform mechanical force $\sigma_{33}(x_1, h) = p_0$. To determine the optimum design of the functionally graded piezoelectric sensors, it is necessary to determine the composition profile that will give the large induced electric potential at the low stress fields. Among the stress fields, the in-plane stress σ_{11} and transverse shear stress σ_{12} are the main cause for the failure of piezoelectric sensors and actuators. For different boundary

conditions, the maximum magnitude of the in-plane stress, transverse shear stress and the induced electric potential are plotted versus the material property gradient index in Figures 5-7. In these figures, the stress fields and the induced electric potential are normalized as the below:

$$\overline{\sigma}_{ij} = \sigma_{ij} / p_0 \quad , \quad \overline{\varphi} = \varphi / p_0$$

It can be observed from Figures 5-7 that for every arbitrary material property gradient index *a*, the maximum magnitude of the in-plane stress, transverse shear stress and the induced electric potential of the functionally graded piezoelectric beams increase with the increase of the length to thickness ratio. This phenomenon can be interpreted as the follow. With the increase of the length to thickness ratio, the bending stiffness of the functionally graded piezoelectric beam reduces. Thus, under a similar mechanical force, the deflection of a slender functionally graded piezoelectric beam will be more than a thick one. Consequently, the values of stresses and the induced electric potential in a slender functionally graded piezoelectric beam will be more than a thick one. This phenomenon is independent of the mechanical boundary conditions.

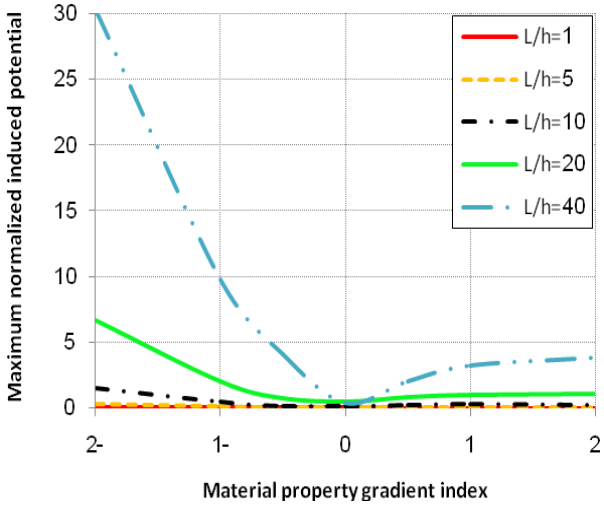

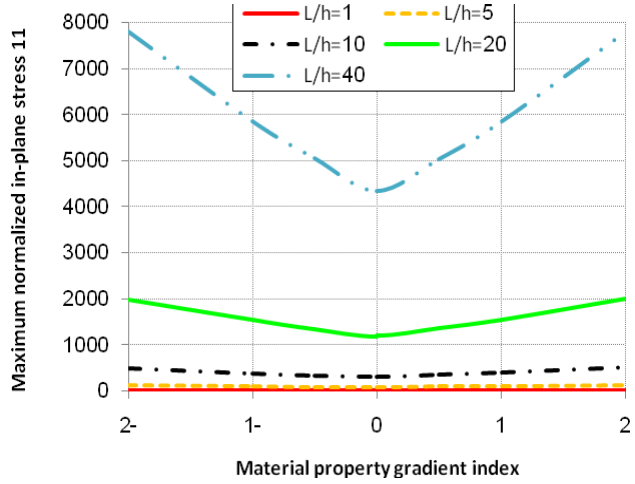

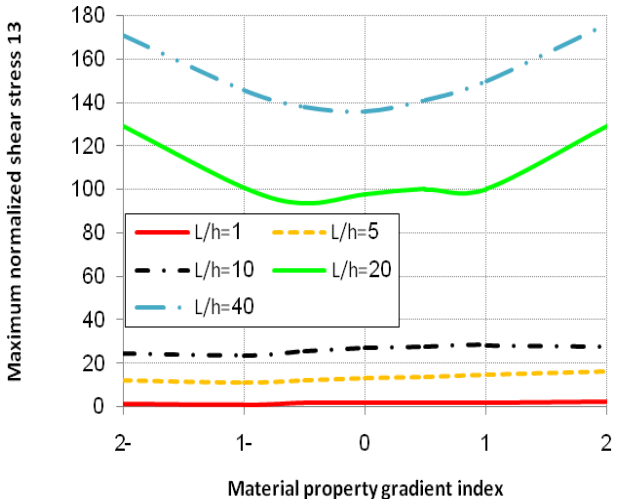

Figure 5. Maximum magnitude of the stress fields and the induced electric potential versus the various material property gradient indexes for the functionally graded piezoelectric sensors with C-F end conditions

It is seen from Figure 5 that in the cantilever functionally graded piezoelectric beams with $a<0$, the induced electric potential increases sharply with the decrease of the material property gradient index. Such behavior can be interpreted using the coupled electromechanical properties of piezoelectric materials. Under mechanical loadings, the soft piezoelectric materials undergo more mechanical deformations and consequently convert more mechanical energy into the electrical energy. For $a>0$, the induced electric potential increases slightly with the increase of the material property gradient index, then the induced electric potential stabilizes and converges to a constant value. The intensity of this phenomenon is more pronounced in the slender graded piezoelectric beams. The maximum value of the transverse shear stress increases with increasing of the material property gradient index. The in-plane stress σ_{11} takes its minimum value when $a=0$. According to these obtained numerical results, it can be concluded that the optimum design of the cantilever functionally graded piezoelectric sensors can be achieved when the material property gradient index is less than -0.7. Indeed, the selection of a volume fraction distribution less than -0.7 leads to inducing the large electric potential in a functionally graded piezoelectric sensor at the low stress fields. It can be also deduced from Figures 5 that the thin functionally graded piezoelectric beams are more efficient sensors than thick one. Although the values of stress fields in the slender functionally graded piezoelectric sensors are higher than thick sensors, the electric potential induced in the slender sensors are also higher than thick ones.

Concerning the functionally graded piezoelectric beams with S-S and C-C end conditions, the variations of the induced electric potential and the in-plane stress with respect to the material property gradient index are the same as the graded piezoelectric beams with C-F end conditions. It must be pointed out that as it expected, the boundary conditions influence the electromechanical response of functionally graded piezoelectric beams. For more clarity, the in-plane stress contours corresponding to functionally graded piezoelectric sensors with different end conditions are shown in Figure 8 for a=-2 and S=5. However, the obtained numerical results reveal that the maximum magnitude of the in-plane stress, transverse shear stress and the induced electric potential versus the material property gradient index are not affected by the mechanical boundary conditions, whatever the length to thickness ratio. In contrast to the cantilever functionally graded beams, the maximum value of the transverse shear stress in the functionally graded piezoelectric beams with S-S and C-C end conditions is independent of the variations of the material property gradient index. It seems that the selection of a material property gradient index less than -1 is the most suitable volume fraction distribution for the functionally graded piezoelectric sensor with S-S and C-C end conditions. Similar to the cantilever functionally graded piezoelectric beams, the thin functionally graded piezoelectric beams are more efficient sensors than thick one.

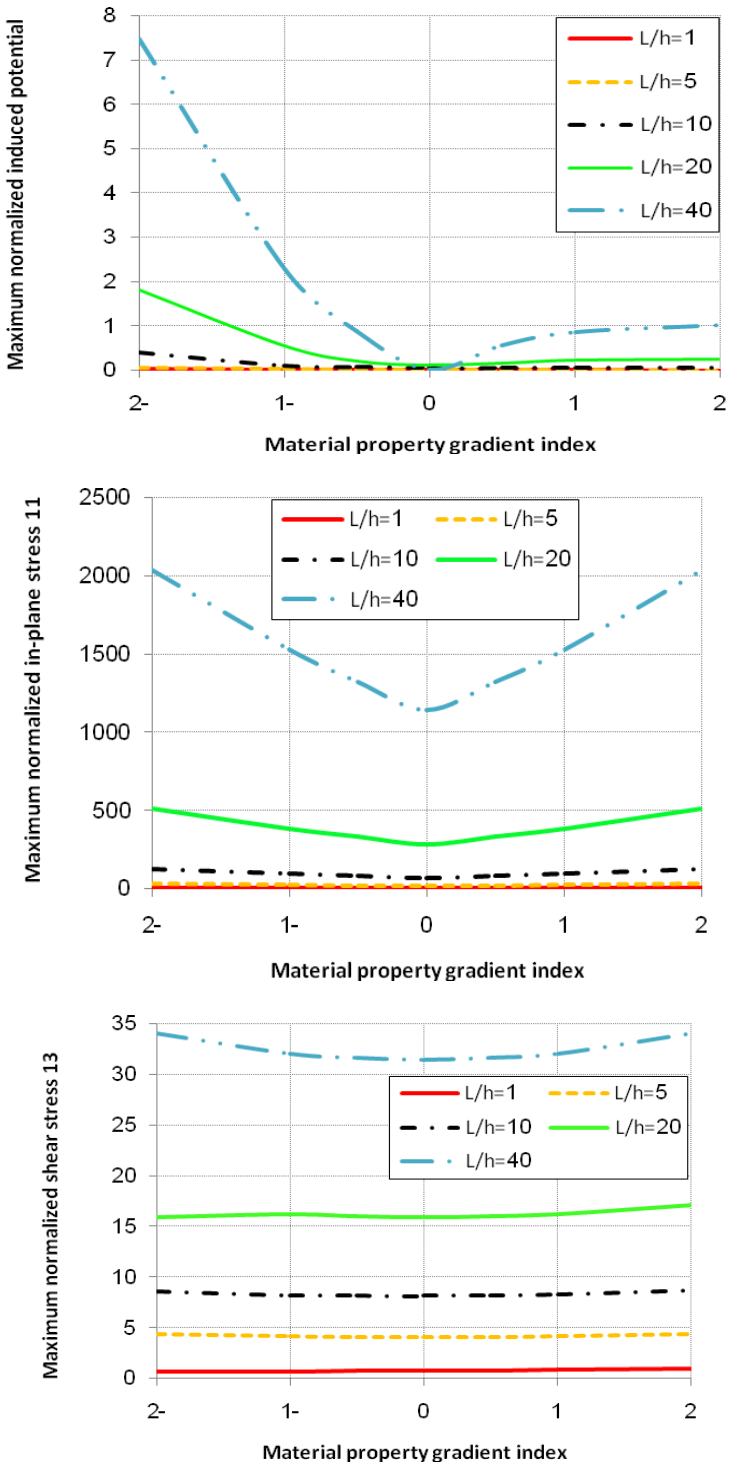

Figure 6. Maximum magnitude of the stress fields and the induced electric potential versus the various material property gradient indexes for the functionally graded piezoelectric sensors with S-S end conditions

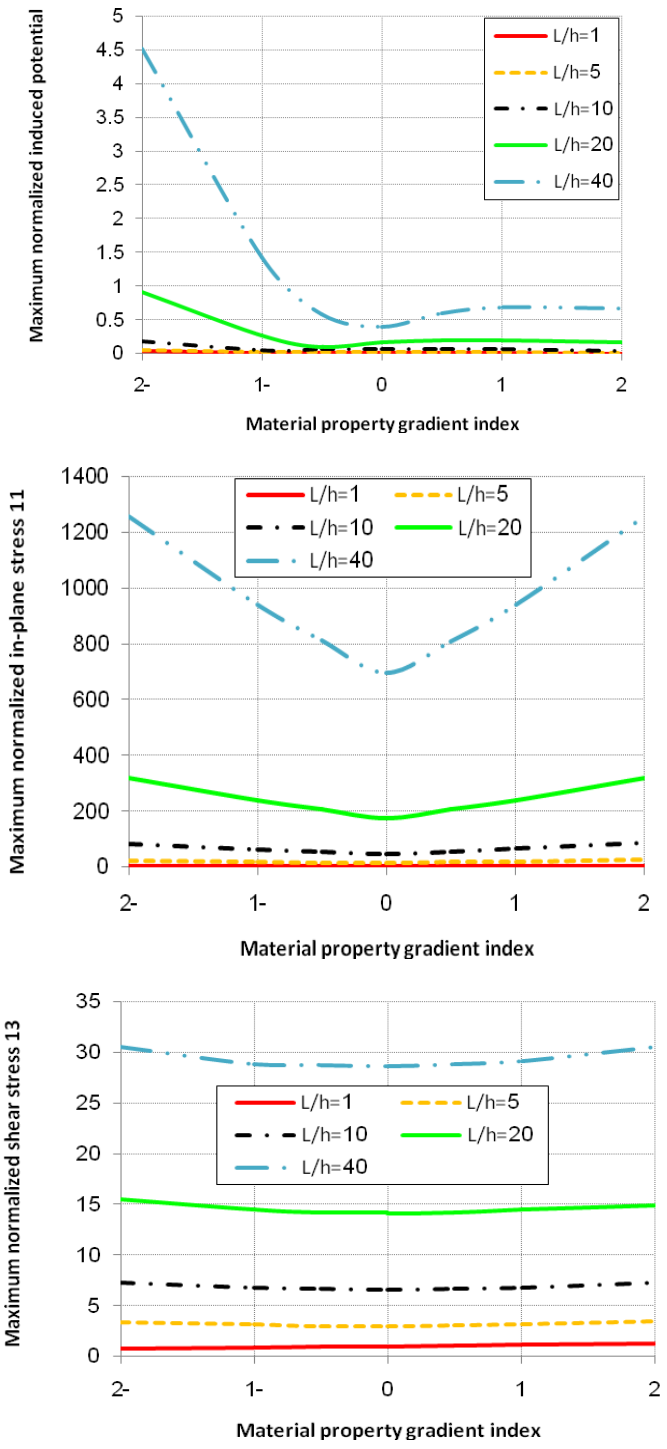

Figure 7. Maximum magnitude of the stress fields and the induced electric potential versus the various material property gradient indexes for the functionally graded piezoelectric sensors with C-C end conditions

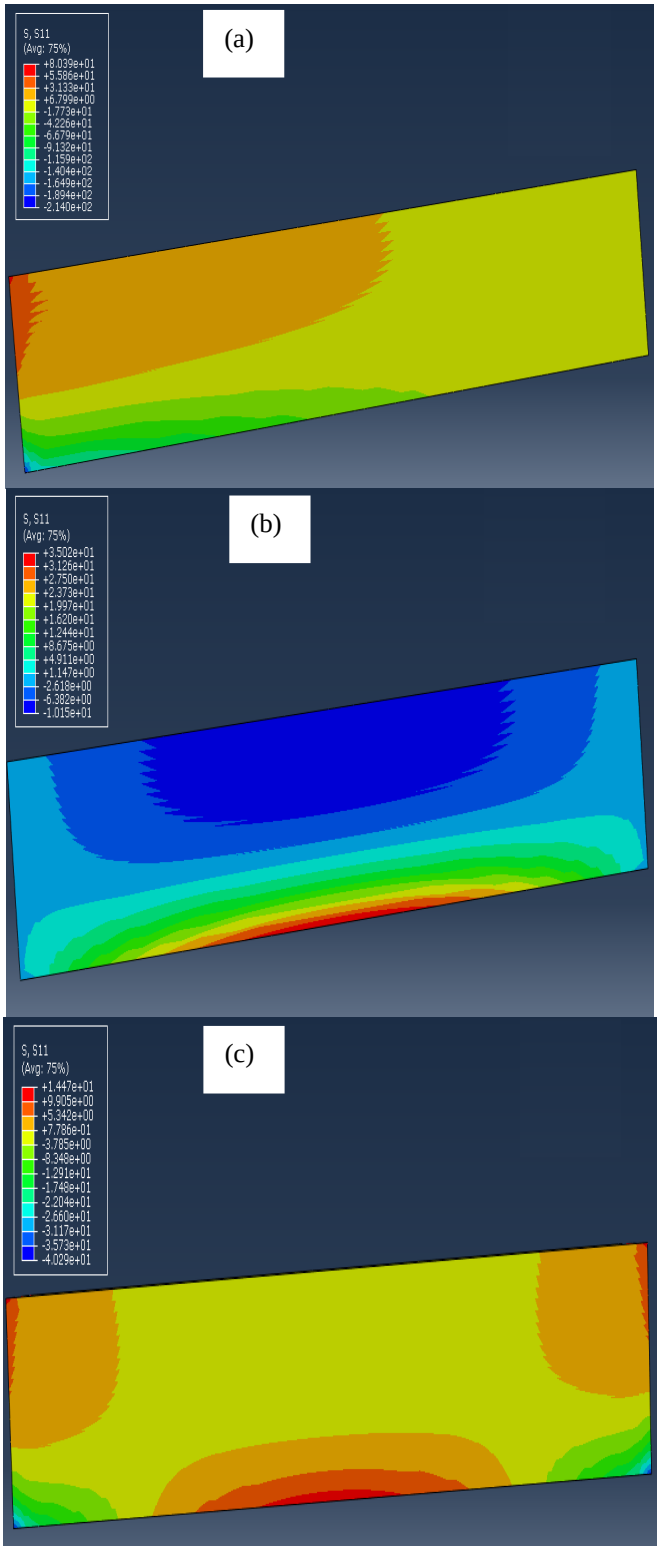

Figure 8. The in-plane stress contours for the functionally graded piezoelectric sensors (a=-2 and S=5) with different end conditions: (a) clamped-free, (b): simply support, (c): clamped-clamped.

In the next case, the uniform electric potential $\phi(x_1, h) = \phi_0$ is applied to the top of the functionally graded piezoelectric beams. In order to achieve the optimum design of the functionally graded piezoelectric actuators, it is necessary to determine the composition profile that will give the large deflection at the low stress fields. To reach this aim, the maximum magnitude of the stress fields and the transverse displacement are plotted as a function of the material property gradient index *a* in Figures 9-11 for

the functionally graded piezoelectric beams with different end conditions. In these figures, the stress fields and the induced electric potential are normalized as the below:

$$\bar{\sigma}_{ij} = \sigma_{ij} / \varphi_0 \quad , \quad \bar{u}_i = u_i / \varphi_0$$

For different boundary conditions, it can be observed from Figures 9-11 that the transverse bending displacement increases with the increasing of the magnitude of the material property gradient index. On the other hand, the maximum values of the in-plane and transverse shear stresses increase with increasing of the material property gradient index. In order to achieve a functionally graded piezoelectric actuator which produces large deflection at the low stress fields, the material property gradient index must be selected a large negative value. On the other words, the soft gradient piezoelectric materials are the most effective selection for the design of the functionally graded piezoelectric actuators. It is also deduced from Figures 9-11 that the thin functionally graded piezoelectric beams are more efficient actuators than thin ones. By increasing the length to thickness ratio not only the produced deflection of the functionally graded piezoelectric actuators increases but also their stress fields reduce.

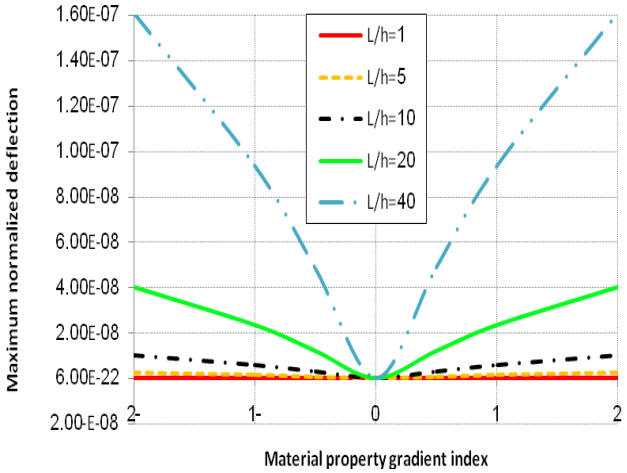

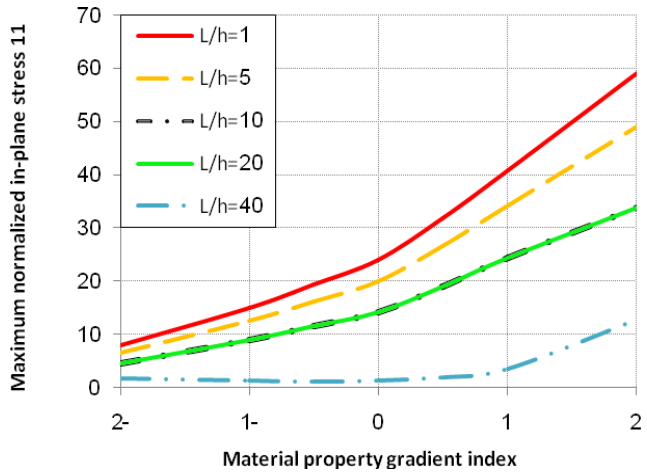

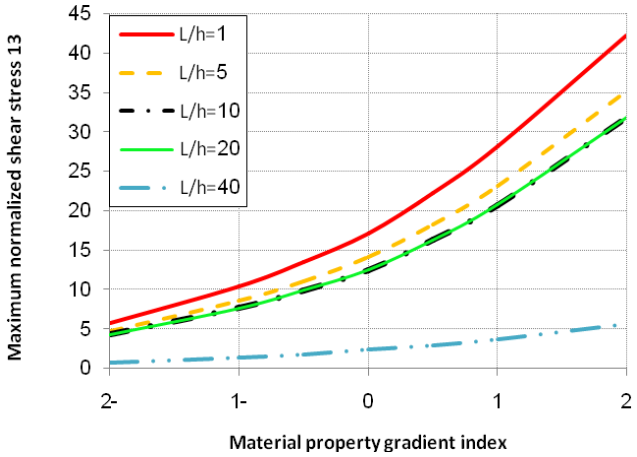

Figure 9. Calculated maximum magnitude of the stress fields and the transverse displacement for the cantilever functionally graded piezoelectric actuators with various material property gradient indexes

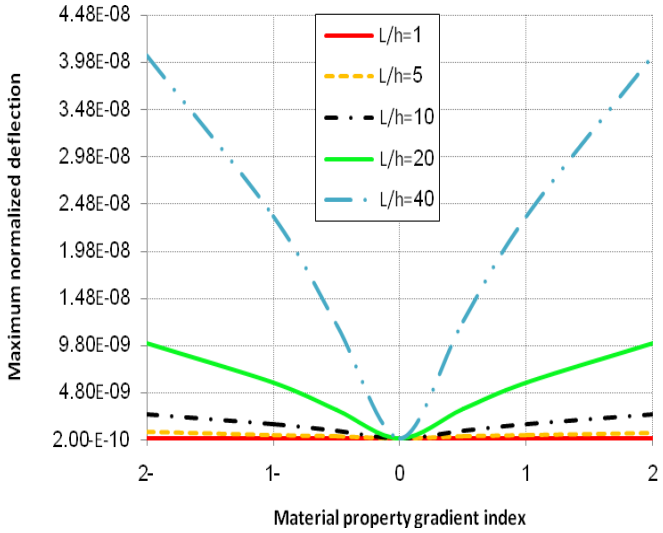

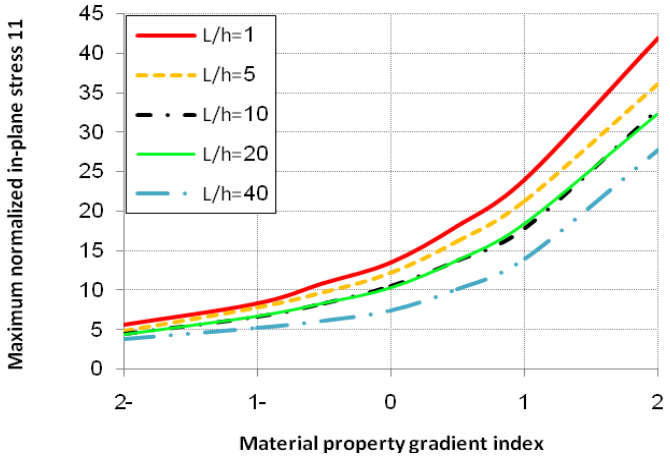

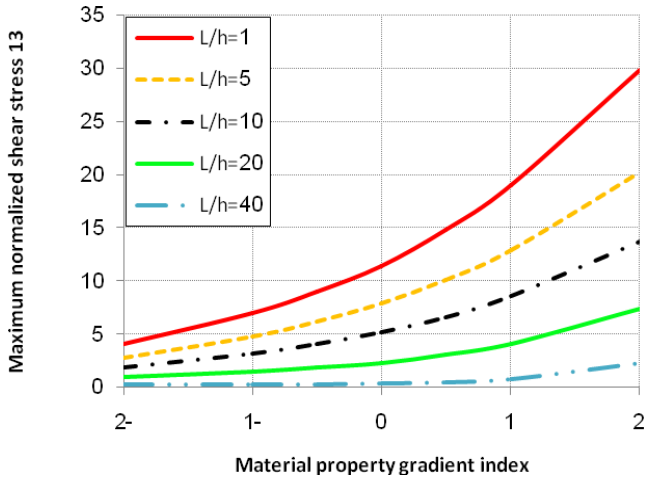

Figure 10. Calculated maximum magnitude of the stress fields and the transverse displacement for the simply supported functionally graded piezoelectric actuators with various material property gradient indexes

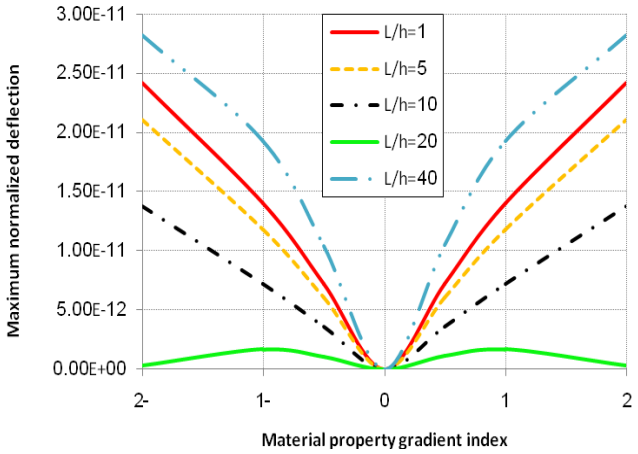

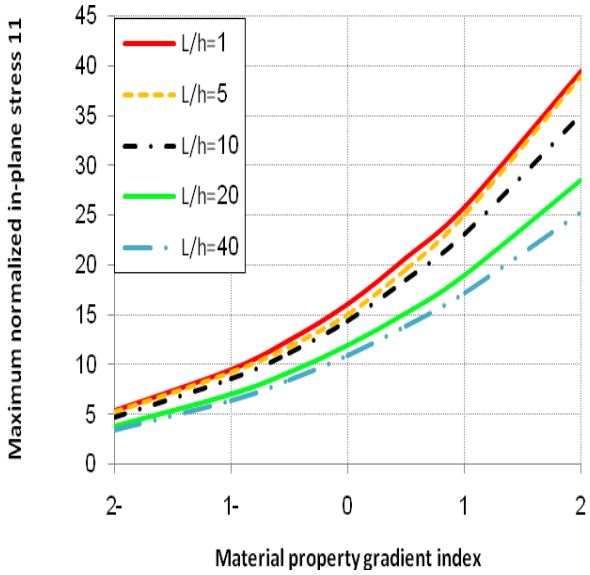

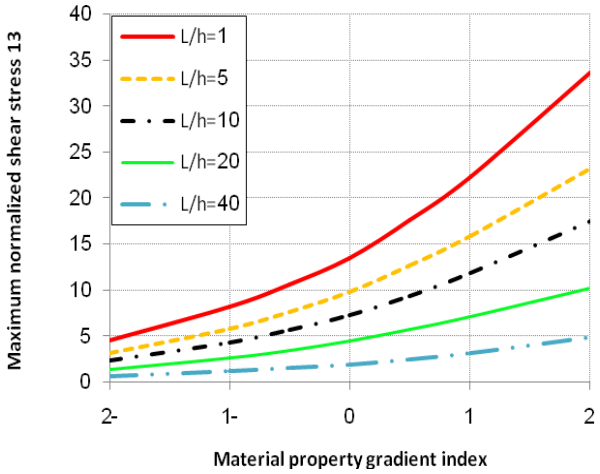

Figure 11. Calculated maximum magnitude of the stress fields and the transverse displacement for the clamped-clamped functionally graded piezoelectric actuators with various material property gradient indexes

7. Conclusions

The relation between different functionally gradient material properties and the optimum sensing/actuation design of the functionally graded piezoelectric beams, i.e. large bending\sensing while reducing the induced stress fields has been investigated in this study. To this end, 3D finite element analysis has been employed. Various static electro-mechanical tests for functionally graded piezoelectric beams with different geometric parameters, material gradient index, mechanical and electrical boundary conditions are carried out. According to the numerical results obtained in the present study, the following main results can be concluded:

1) The optimum design of the functionally graded piezoelectric sensors can be achieved when a value less than –1 is selected for the material property gradient index.
2) The thin functionally graded piezoelectric beams are more efficient sensors than thick ones.
3) The maximum value of the transverse shear stress in the functionally graded piezoelectric sensors with S-S and C-C end conditions is independent of the variations of the material property gradient index.
4) The soft gradient piezoelectric materials are the most effective selection for the design of the functionally graded piezoelectric actuators.
5) The thin functionally graded piezoelectric beams are more efficient actuators than thick ones.
6) For the functionally graded piezoelectric beams under the action of electrical loadings, the maximum values of the in-plane and transverse shear stresses increase with the increase of the material property gradient index.

References

Bathe, K. J., 1982. Finite element procedures in engineering analysis, Englewood Cliffs, NJ: Prentice-Hall.

Benjeddou, A., 2000. Advances in piezoelectric finite element modeling of adaptive structural elements: a survey, *Computers & Structures*, Vol. 76, pp. 347-363.

Behjat, B., Salehi, M., Sadighi, M., Armin, A. and Abbasi, M., 2009. Static, dynamic, and free vibration analysis of functionally graded piezoelectric panels using finite element method, *Journal of Intelligent Material Systems and Structures*, Vol. 20, pp. 1635-1646.

Behjat, B., Salehi, M., Sadighi, M., Armin, A. and Abbasi, M., 2011. Static Static and dynamic analysis of functionally graded piezoelectric plates under mechanical and electrical loading, *Scientia Iranica, Transactions B: Mechanical Engineering*, Vol. 18, No. 4, pp. 986-994.

Beheshti-Aval, S. B. and Lezgy-Nazargah, M., 2010a. A finite element model for composite beams with piezoelectric layers using a sinus model, *Journal of Mechanics*, Vol. 26, No. 2, pp. 249-258.

Beheshti-Aval, S. B. and Lezgy-Nazargah, M., 2010b. Assessment of velocity-acceleration feedback in optimal control of smart piezoelectric beams, *Smart Structures and Systems*, Vol. 6, No. 8, pp. 921-938.

Beheshti-Aval, S. B., Lezgy-Nazargah, M., Vidal, P. and Polit, O., 2011. A refined sinus finite element model for the analysis of piezoelectric laminated beams, *Journal of Intelligent Material Systems and Structures*, Vol. 22, pp. 203-219.

Beheshti-Aval, S. B. and Lezgy-Nazargah, M., 2012a. A coupled refined high-order global-local theory and finite element model for static electromechanical response of smart multilayered/sandwich beams, *Archive of Applied Mechanics*, Vol. 82, No. 12, pp. 1709-1752.

Beheshti-Aval, S. B. and Lezgy-Nazargah, M., 2012b. Coupled refined layerwise theory for dynamic free and forced response of piezoelectric laminated composite and sandwich beams, *Meccanica*, doi: 10.1007/s11012-012-9679-2.

Bodaghi, M. and Shakeri, M., 2012. An analytical approach for free vibration and transient response of functionally graded piezoelectric cylindrical panels subjected to impulsive loads, *Composite Structures*, Vol. 94, pp. 1721-1735.

Bodaghi, M., Damanpack, A. R., Aghdam, M. M. and Shakeri, M., 2012. Non-linear active control of FG beams in thermal environments subjected to blast loads with integrated FGP sensor/actuator layers. *Composite Structures*, Vol. 94, pp. 3612-3623.

Delale, F. and Erdogan, F., 1988. On the mechanical modeling of the interfacial region in bonded half planes, *ASME Journal of Applied Mechanics*, Vol. 55, pp. 317–324.

D'Ottavio, M. and Polit, O., 2009. Sensitivity analysis of thickness assumptions for piezoelectric plate models, *Journal of Intelligent Material Systems and Structures*, Vol. 20, No. 15, pp. 1815-1834.

Erdogan, F., 1985. The crack problem for bonded nonhomogeneous materials under antiplane shear loading, *ASME Journal of Applied Mechanics*, Vol. 52, pp. 823–828.

Gu, P. and Asaro, J., 1997. Crack in functionally graded materials, *International Journal of Solids and Structures*, Vol. 34, pp. 1–17.

Lee, H. J., 2005. Layerwise laminate analysis of functionally graded piezoelectric bimorph beams, *Journal of Intelligent Material Systems and Structures*, Vol. 16, pp. 365-371.

Lezgy-Nazargah, M., Vidal, P. and Polit, O., 2013. An efficient finite element model for static and dynamic analyses of functionally graded piezoelectric beams, *Composite Structures*, Vol. 104, pp. 71-84.

Li, Y. and Shi, Z., 2009. Free vibration of a functionally graded piezoelectric beam via state-space based differential quadrature, *Composite Structures*, Vol. 87, pp. 257-264.

Lim, C. W. and He, L. H., 2001. Exact solution of a compositionally graded piezoelectric layer under uniform stretch, bending and twisting, *International Journal of Mechanical Science*, Vol. 43, pp. 2479-2492.

Lu, P., Lee H. P. and Lu, C., 2005. An exact solution for functionally graded piezoelectric laminates in cylindrical bending, *International Journal of Mechanical Science*, Vol. 47, pp. 437-458.

Lu, P., Lee H. P. and Lu, C., 2006. Exact solutions for simply supported functionally graded piezoelectric laminates by Stroh-like formalism, *Computers & Structures*, Vol. 72, pp. 352-363.

Liu, T. T. and Shi, Z. F., 2004. Bending behavior of functionally gradient piezoelectric cantilever, *Ferroelectrics*, Vol. 308, pp. 43-51.

Noda, N. and Jin, Z. H., 1993. Thermal stress intensity factors for a crack in a strip of a functionally gradient material, *International Journal of Solids and Structures*, Vol. 30, pp. 1039–1056.

Niezrecki, C., Brei, D., Balakrishnan, S. and Moskalik, A., 2001. Piezoelectric actuation: state of the art, *Shock and Vibration Digest*, Vol. 33, No. 4, pp. 269-80.

Pablo, F., Bruant, I. and Polit, O., 2009. Use of classical plate finite elements for the analysis of electroactive composite plates: numerical validations, *Journal of Intelligent Material Systems and Structures*, Vol. 20, No. 15, pp. 1861-1873.

Reddy, J. N. and Cheng, Z. Q., 2001. Three-dimensional solutions of smart functionally graded plates, *ASME* Journal of Applied Mechanics, Vol. 68, pp. 234-241.

Shi, Z. F. and Chen, Y., 2004. Functionally graded piezoelectric cantilever beam under load, *Archive of Applied Mechanics*, Vol. 74, pp. 237-247.

Tzou, H. S. and Tseng, C. I., 1990. Distributed piezoelectric sensor/actuator design for dynamic measurement /control of distributed parameter systems: a piezoelectric finite element approach, *Journal of Sound and Vibration*, Vol. 138, No. 1, pp. 17-34.

Vidal, P., D'Ottavio, M., Thaier M. B. and Polit, O., 2011. An efficient finite shell element for the static response of piezoelectric laminates, *Journal of Intelligent Material Systems and Structures*, Vol. 22, No. 7, pp. 671-690.

Wu, X. H., Chen, C. Q. and Shen, Y. P., 2002. A high order theory for functionally graded piezoelectric shells, *International Journal of Solids and Structures*, Vol. 39, pp. 5325-5344.

Wu, C. C. M., Kahn M. and Moy, W., 1996. Piezoelectric ceramics with functional gradients: a new application in material design, *Journal of American Ceramic Society*, Vol. 79, pp. 809-12.

Xiang, H. J. and Shi, Z. F., 2009. Static analysis for functionally graded piezoelectric actuators or sensors under a combined electro-thermal load, *European Journal of Mechanics: A Solids*, Vol. 28, pp. 338-346.

Yang, J. and Xiang, H. J., 2007. Thermo-electro-mechanical characteristics of functionally graded piezoelectric actuators, *Smart Materials and Structures*, Vol. 16, pp. 784-797.

Zhong, Z. and Shang, E. T., 2003. Three-dimensional exact analysis of a simply supported functionally gradient piezoelectric plate, *International Journal of Solids and Structures*, Vol. 40, pp. 5335-5352.

Zhu, X. H. and Meng, Z. Y., 1995. Operational principle, fabrication and displacement characteristic of a functionally gradient piezoelectric ceramic actuator, *Sensors and Actuators: A*, Vol. 48, pp. 169-76.

Biographical notes

Mojtaba Lezgy-Nazargah received the B.S degree in Civil Engineering from Shahrood University of Technology, Shahrood, Iran in 2006. He received his M.S. and Ph.D. degrees in Civil and Structural Engineering from K.N. Toosi University of Technology, Tehran, Iran in 2008, 2011 respectively. He has been working as Assistant Professor in the Civil Engineering Department at Hakim Sabzevari University, Sabzevar, Iran, since 2011. His major research interests include "computational mechanics", "active vibration control of structures", "smart materials and structures", "laminated composite structures", "nonlinear analysis of steel and reinforced concrete structures". He has published more than 10 papers in the international journals. He has also written a book for design of reinforced concrete structures in Persian. Dr. Lezgy-Nazargah has supervised 11 B.S. and. M.S. research work in his research areas. He teaches courses on "Static", "Mechanics of Materials", "Finite Element Analysis", "Theory of Elasticity", "Plates and Shells" and "Design of Reinforced Concrete Structures".

Mostafa Farahbakhsh was born in Tabas, Iran, in 1991. In 2009, he entered the Civil Engineering program at Hakim Sabzevari University, Sabzevar, Iran and obtained his B.S. degree in Civil Engineering in 2013. His B.S. degree studies included an ''Investigation of Electro-Mechanical Behavior of Functionally Graded Piezoelectric Materials by Finite Element Method", under the supervision of Dr. Mojtaba Lezgy-Nazargah. Mostafa Farahbakhsh was also teaching assistant in the area of ''Static" and "Design of Reinforced Concrete Structures". Mostafa Farahbakhsh's research interests have focused on: reinforced concrete structures, functionally graded materials, smart materials and structures.

Received April 2013
Accepted May 2013
Final acceptance in revised form July 2013